L-Shell Absorption Spectrum of an Open-M-Shell Germanium Plasma: Comparison of Experimental Data with a Detailed Configuration-Accounting Calculation

J. M. Foster, D. J. Hoarty, C. C. Smith, P. A. Rosen, and S. J. Davidson
Atomic Weapons Establishment, Aldermaston, Reading RG7 4PR, United Kingdom

S. J. Rose
Rutherford Appleton Laboratory, Chilton, Didcot OX11 0QX, United Kingdom

T. S. Perry and F. J. D. Serduke
Lawrence Livermore National Laboratory, P.O. Box 808, Livermore, California 94550
(Received 29 July 1991)

The radiative opacity of a near local thermodynamic equilibrium, open-M-shell Ge plasma has been measured in the region of the $2p$-$3d$ and $2p$-$4d$ transition arrays, and is compared for the first time with the results of a detailed configuration-accounting calculation which includes an approximate treatment of term widths. The plasma was generated by radiation heating using thermal x radiation from a laser-produced gold plasma. Temperature and density were characterized in experiments which observed the absorption spectra of Al and Mg plasmas and by radiographic measurements of the expansion of the heated foil samples.

PACS numbers: 52.25.Nr, 52.50.Jm, 52.70.La

Heating of sample materials by the thermal radiation from a laser-produced plasma has been used [1–4] as a means of creating hot, dense plasmas whose radiative opacity may be measured by absorption spectroscopy. High density ensures that collisional processes dominate the ionization and excitation of the plasma while the imposed radiation field largely offsets the effect of radiative losses. These experiments thus create near local thermodynamic equilibrium (LTE) plasmas and provide valuable data which may be used to test approximations made in opacity calculations.

We have shown previously [1,2] the comparison of experimental data for the opacity of an open-L-shell aluminum plasma with the results of an approximate calculation. Recently, more fully detailed term-accounting calculations [5] reproduce the experimental absorption spectra with excellent agreement. In the case of materials with an open-M-shell detailed term, accounting is, in general, impractical because the prohibitively large number of individual lines and opacity calculations are by necessity approximate. They attempt to include enough detail to provide reliable estimates of mean opacities (to be used, for example, in radiation flow calculations) and detailed configuration-accounting (DCA) calculations or, more simply, average-atom prescriptions are commonly used [6–8]. Calculations of spectral structure based on a limited set of configurations may include all the term structure and be useful for diagnostic purposes [2,4].

In this Letter we describe measurements of the radiative opacity of an open-M-shell (germanium) plasma, and present the first comparisons of experimental data with the results of a DCA opacity code calculation which treats term structure in an approximate manner using the unresolved transition array approach.

The experimental arrangement is shown schematically in Fig. 1. Thin foil samples of the material of interest are indirectly heated using thermal x radiation from separate laser-produced plasmas created by focusing the two main beams of the Atomic Weapons Establishment (AWE) HELEN Nd-glass laser onto gold targets (each beam delivering up to 220 J of energy at 0.53-μm wavelength in a 200-ps duration pulse). The target geometry is arranged to achieve uniform illumination of the sample by

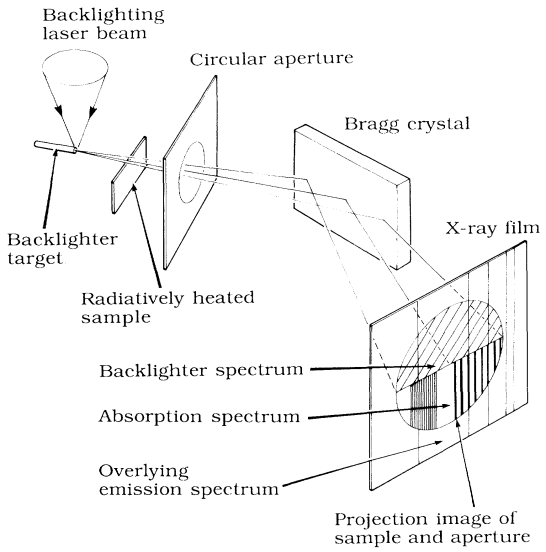

FIG. 1. Schematic of the experimental arrangement used to measure the absorption spectrum of a radiatively heated germanium plasma.

x radiation and to prevent its direct illumination by laser light. The foil sample is coated on both faces with Parylene-N which tamps its expansion and keeps the entire sample mass contained and homogeneous. The thickness of the sample is chosen to give an optical depth close to unity in the region of interest in the spectrum. The tamper thickness is chosen as that which (in hydrocode calculations of the experiment) results in uniform density ($< 10\%$ variation between center and outer face) throughout the heated, expanded sample material at the time when its absorption spectrum is recorded. In the present experiment a sample foil of 3000-Å thickness of germanium tamped by 1-μm thickness of Parylene-N on both sides was used. The HELEN backlighter beam (50 J at 0.53-μm wavelength in a 200-ps pulse) is used to illuminate a small (typically 20 μm) diameter glass fiber target coated with approximately 1-μm thickness of a rare-earth metal (neodymium in the case of the germanium sample experiment) chosen so that its laser-plasma emission spectrum falls in the spectral region of interest. This short-duration, near-point backlighting source, the heated sample, and an appropriate circular aperture are arranged together with a Bragg crystal spectrometer in the point-projection-spectroscopy geometry [9,10] so that the unattenuated and attenuated backlighter spectra, together with the overlying emission spectrum of the sample, may all be recorded simultaneously on x-ray sensitive film (Fig. 2). A spectral resolution of approximately 1.5 eV is achieved in the present germanium opacity experiment where a RbAP Bragg crystal is used. The backlighter target is illuminated at typically 700-ps delay relative to the main beams; at this time the electron temperature and density of the heated sample are approximately 80 eV and 0.01 times original solid density. The x-ray film data are processed using a digitizing microdensitometer, the overlying emission spectrum is subtracted from the unattenuated and attenuated backlighter spectra, and division of these yields the absorption spectrum of the sample material.

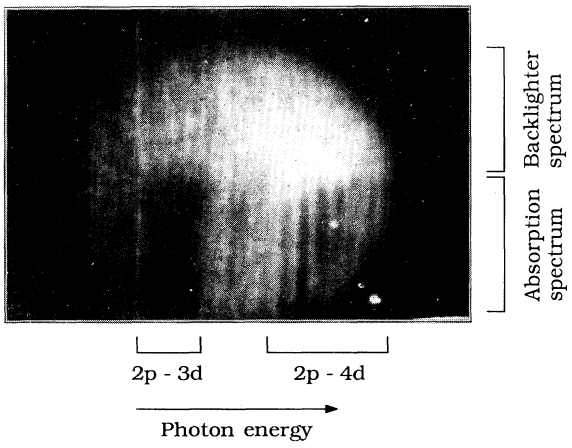

FIG. 2. X-ray film record showing the point-projection image of the sample and circular aperture, the neodymium backlighter spectrum and germanium absorption spectrum, and the overlying weak emission spectrum.

We have characterized the thermal x-ray emission from the laser-produced gold plasmas which heat the sample by using an array of filtered vacuum x-ray diodes. The x-ray heating flux at the sample was calculated from these measurements and the geometry of the target. An effective drive temperature (proportional to the one-quarter power of this flux) was used as input to the AWE one-dimensional Lagrangian hydrocode NYM [11] in simulations of the sample heating and expansion. This obviated the need to model the laser-plasma interaction.

We have benchmarked these simulations of sample heating in experiments using aluminum and magnesium plasmas for which detailed term-accounting calculations are practicable. We make comparison of the observed aluminum $1s$-$2p$ absorption spectrum with calculation [1,2,5] and identify combinations of temperatures and density which reproduce the experimental data. This comparison is sensitive to 5-eV variations of temperature (at constant density) and factor-of-2-variations of density (at constant temperature). In addition, we have made direct measurements of sample density by radiographic measurement of the expansion of heating magnesium foil samples, and by measurement of the Stark-broadened widths of heliumlike magnesium lines where they merge with the continuum [12]. Density can be deduced with better than factor-of-2 accuracy from the measured line shapes, and with $\pm 20\%$ accuracy from the measurement of foil expansion. Hydrocode calculations of these experiments typically show small departures of temperature and density from those which reproduce the experimental data, and we consequently modify the radiation drive assumed in the hydrocode calculation by use of a multiplier of the effective drive temperature. By this means, with a drive-temperature multiplier of 0.9, the experimental data and calculation are brought into rather close agreement.

A typical experimental absorption spectrum for a germanium plasma at 76-eV temperature and 0.05-g cm^{-3} density is shown in Fig. 3. The quoted temperature and density are those calculated in a NYM hydrocode calculation using the 0.9 multiplier of the effective drive temperature. The main features of the spectrum, labeled in Fig. 3, were identified by comparison with calculations of line strengths and transition energies using a multiconfiguration Dirac-Fock atomic structure code [13] for some of the simpler configurations. The germanium absorption spectrum shows a clear "picket-fence"-like structure in the (overlapping) $2p_{3/2}$-$4d_{5/2}$ and $2p_{1/2}$-$4d_{3/2}$ groups of lines. The transmission minima are associated with different total numbers of bound M-shell electrons. In the case of the $2p$-$3d$ lines an analogous picket-fence profile is not visible, although the optical depth in this part of the spectrum is rather large in the data of Fig. 3.

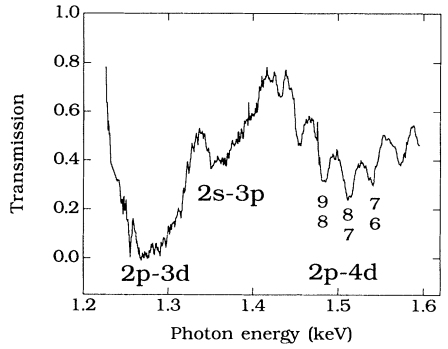

FIG. 3. Absorption spectrum of a 1.6×10^{-4}-g cm^{-2} germanium plasma at 76-eV temperature and 0.05-g cm^{-3} density. The numbers labeling the transmission minima are the total number of bound M-shell electrons in configurations giving rise to $2p_{1/2}$-$4d_{3/2}$ (upper figures) and $2p_{3/2}$-$4d_{5/2}$ (lower figures) transition arrays.

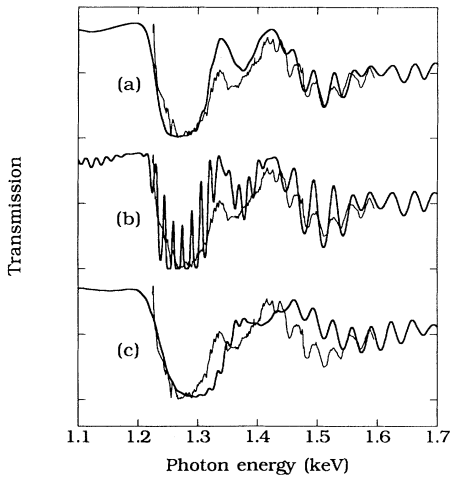

FIG. 4. Calculated transmission (bold lines) of the germanium plasma compared with experiment (faint lines) for three schemes of modeling configuration abundance and term widths (see text).

We have also carried out experiments in which the original (solid density) thickness of the germanium sample was 500 Å (to be compared with 3000 Å for the data of Fig. 3), and in these experiments the $2p$-$3d$ line cluster also showed a smooth profile.

We compare our experimental data for the germanium absorption spectrum with synthetic absorption spectra calculated using the known sample area density and the frequency-dependent opacity obtained from an opacity code (IMP) developed at the Rutherford Appleton Laboratory.

The IMP opacity code is described in detail elsewhere [14]. In brief summary, the model starts with the solution of the Dirac equation in the Thomas-Fermi average-atom potential and the calculation of average one-electron properties (orbital energies, oscillator strengths, and bound-free oscillator density). The principal quantum shells are categorized as "core" (full or almost full), "valence" (open), and "Rydberg" (almost empty or empty). All possible electron configurations with full core and empty Rydberg orbitals are constructed in a relativistic representation. The splitting of each configuration energy into its terms (levels of different total angular momentum, J) is not calculated explicitly, but treated approximately by representing transition arrays between pairs of configurations by a Gaussian line (of width defined here as the "term width") as described by Moszkowski [15]. In addition, broadening by inclusion of satellite lines which result from spectator-electron occupancy of the Rydberg orbitals is included by adding a further Gaussian width ("dielectronic width") to the line, as described by Goldberg and Rozsnyai [16]. Configuration-to-configuration transitions, with energies and oscillator strengths calculated from the one-electron properties, are thus represented as single Gaussian lines whose widths are given by the quadratic sum of the term and dielectronic widths. Doppler broadening is also included; other broadening mechanisms are not. Valence shell configurations are populated by either of two methods. "Method 1" uses the Saha-Boltzmann equations with configuration energies derived from the appropriate radial integrals of the wave functions. "Method 2" is that described by Carson, Mayers, and Stibbs [17] in which configuration abundances are calculated as the product of probabilities of subshell occupancies, each of which has a binomial distribution. It implicitly assumes that orbital occupancies are not statistically correlated.

We show in Fig. 4 simulations of the experimental germanium absorption spectrum which were calculated for the following schemes of modeling of configuration abundance and term width: (a) method 1 and Moszkowski model for term widths, (b) method 1 and term widths not included, and (c) method 2 and Moszkowski model for term widths; the dielectronic width was included in all cases. The $2p$-$3d$ absorption feature is predicted to be unresolved (in agreement with experiment) in the calculation which includes an approximate treatment of term widths, and the $2p$-$4d$ feature shows considerable structure in agreement with experiment. In the case of the calculation which uses Saha-Boltzmann statistics (method 1) in the calculation of configuration abundances, experiment and calculation are in rather close agreement, although in the case of the method-2 approximation, the overall widths of the $2p$-$3d$ and $2p$-$4d$ groups of lines are seen to be greater (higher abundance of configurations remote from the average ion) because of neglect of statistical correlations. All the synthetic spectra of Fig. 4 have been shifted to lower photon energy by a small amount (20 eV) to improve agreement with experiment—this is thought to be necessary because IMP uses an approximate (Thomas-Fermi) potential [14]. The

difference in ionization apparent between the two methods of calculation is an anomaly arising from the use of total configuration energies in the full Saha-Boltzmann calculation, whereas one-electron eigenvalues were used to derive orbital occupation probabilities for the binomial distributions. This difference would disappear if the atomic potential, in which the wave equation is solved, were iterated to self-consistency.

In summary, we have measured the frequency-dependent radiative capacity of an open-M-shell germanium plasma, and described the first comparisons with calculations using a configuration-accounting opacity code in which term widths are approximately included. Comparison of experiment and simulation highlights the importance of (a) term widths in determining the distribution of line transitions within a line cluster under circumstances where the term splitting is comparable to the spacing of lines arising from different (valence shell) configurations, and (b) statistical correlations in the thermal distribution of electron configurations.

We would like to thank Ian Smith, Mark Stevenson, Mike Norman, and other members of the HELEN laser operations team, Roy Powell, Roy Culliford, and other members of the HELEN target chamber team, and Doug Sutton, Tony Tyrrell, and members of the AWE laser target fabrication group, who all significantly contributed to the successful completion of these experiments. Basil Crowley and Daryl Landeg contributed to many helpful discussions, and we are grateful to Jonathan Hansom, who established the image and data processing procedures which were essential in the analysis of the experimental data reported in this Letter.

[1] S. J. Davidson, J. M. Foster, C. C. Smith, K. A. Warburton, and S. J. Rose, Appl. Phys. Lett. **52**, 847 (1988).

[2] S. J. Davidson, C. L. S. Lewis, D. O'Neill, S. J. Rose, J. M. Foster, and C. C. Smith, in *Laser Interaction with Matter,* edited by G. Verlade, E. Minguez, and J. Perlado (World Scientific, Singapore, 1989).

[3] C. Chenais-Popovics, C. Fievet, J. P. Geindre, J.-C. Gauthier, E. Luc-Koenig, J. F. Wyart, H. Pépin, and M. Chaker, Phys. Rev. A **40**, 3194 (1989).

[4] J. Bruneau, C. Chenais-Popovics, D. Desenne, J.-C. Gauthier, J.-P. Geindre, M. Klapisch, J.-P. Le Breton, M. Louis-Jacquet, D. Naccache, and J.-P. Perrine, Phys. Rev. Lett. **65**, 1435 (1990).

[5] J. Abdallah, Jr., and R. E. H. Clark, J. Appl. Phys. **69**, 23 (1991).

[6] E. Nardi and Z. Zinamon, Phys. Rev. A **20**, 1197 (1979).

[7] B. F. Rozsnyai, Astrophys. J. **341**, 414 (1989).

[8] S. J. Rose, in *Radiative Properties of Hot Dense Matter,* edited by J. Davis, C. F. Hooper, R. W. Lee, A. Merts, and B. F. Rozsnyai (World Scientific, Singapore, 1985).

[9] C. L. S. Lewis and J. McGlinchey, Opt. Commun. **53**, 179 (1985).

[10] J. M. Foster, Rev. Sci. Instrum. **59**, 1849 (1988).

[11] P. D. Roberts, AWE report, 1980 (unpublished).

[12] P. T. Springer, T. S. Perry, R. E. Stewart, C. A. Iglesias, F. J. Serduke, B. G. Wilson, R. W. Lee, J. M. Foster, C. C. Smith, D. J. Hoarty, and S. J. Davidson, in Proceedings of the International Workshop on Radiation Transfer Properties of Hot Dense Matter, 1990 (World Scientific, Singapore, to be published).

[13] I. P. Grant, B. J. McKenzie, P. H. Norrington, D. F. Mayers, and N. C. Piper, Comput. Phys. Commun. **21**, 207 (1980).

[14] S. J. Rose (to be published).

[15] S. A. Moszkowski, Prog. Theor. Phys. **28**, 1 (1962).

[16] A. Goldberg and B. F. Rozsnyai, Lawrence Livermore National Laboratory Report No. UCRL-95472, 1986 (unpublished).

[17] T. R. Carson, D. F. Mayers, and D. W. N. Stibbs, Mon. Not. R. Astron. Soc. **140**, 483 (1968).

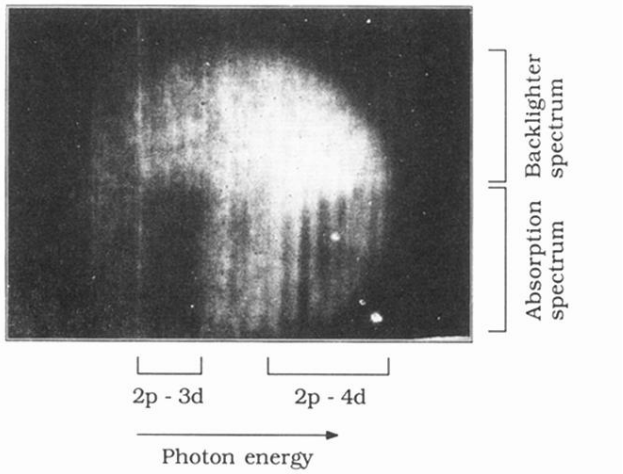

FIG. 2. X-ray film record showing the point-projection image of the sample and circular aperture, the neodymium backlighter spectrum and germanium absorption spectrum, and the overlying weak emission spectrum.